Journal of Catalysis **192,** 174–184 (2000)
doi:10.1006/jcat.2000.2852, available online at http://www.idealibrary.com on IDEAL®

An XRD, XPS, and EPR Study of Li/MgO Catalysts: Case of the Oxidative Methylation of Acetonitrile to Acrylonitrile with CH_4

Catherine L. Bothe-Almquist, Reddy P. Ettireddy, Albert Bobst,[1] and Panagiotis G. Smirniotis[2]

Department of Chemical Engineering, The University of Cincinnati, Cincinnati, Ohio 45221-0171

Received October 5, 1999; revised January 25, 2000; accepted February 17, 2000

The overall purpose of this study was to investigate the effects of the magnesium and lithium precursors and the catalyst surface properties on the catalytic performance in the oxidative methylation of acetonitrile. The performance of the catalysts for the oxidative methylation of acetonitrile to acrylonitrile was significantly affected by the Li precursor, where catalysts prepared with LiCl and LiOH on MgO had the best performance for this reaction. The catalysts' activity was virtually unaffected by the source and surface area of the MgO. In contrast, relatively high BET surface areas appeared to have a negative affect on the catalysts' performance by producing less acrylonitrile and more CO_x. XPS and XRD analyses of Li/MgO-based catalysts indicated that the lithium salts used in the catalyst synthesis predominantly formed mixtures with MgO. It was found that the Li : Cl atomic ratio was 1 : 1 in catalysts prepared with LiCl, even after calcination at 650°C for 14 h in air. XRD analysis of LiCl/MgO catalysts calcined at 650°C suggests that some amount of LiCl precursor on MgO decomposes into Li^+O^- (Li_2O_2). The latter species are believed to be responsible for the effective transformation of methane and acetonitrile to acrylonitrile. The binding energy of Li 1*s* ranges between 57.0 and 52.3 eV. Very interestingly, the binding energy of the Li 1*s* peak observed at 57.0 eV in LiCl/MgO (C1–C6) and LiOH/MgO (C9) catalysts corresponds to Li^+O^- (Li_2O_2). This peak was negligible for Li_2CO_3/MgO (C7 and C8) and $LiNO_3$/MgO (C10) catalysts. Our proposal for this XPS peak of Li^+O^- species is supported by the EPR peak at $g_\perp = 2.0544$. To the best of our knowledge there is no previous communication of the Li 1*s* peak which corresponds to Li^+O^- determined by XPS. Catalytic experiments for the oxidative methylation of acetonitrile to acrylonitrile over the aforesaid catalysts indicate that indeed the catalysts synthesized with LiCl and LiOH promote the desired reaction, or equivalently they are associated with Li^+O^- species. A direct relation between the EPR peak at $g_\perp = 2.0544$ and the lack of CO was established. Although the LiCl/MgO catalysts' performance was better than that of other catalysts prepared in this study, it was also the least stable. Observations made during these studies suggest that lithium sublimation occurs, thus resulting in catalyst deactivation. It is remarkable to note that catalysts synthesized with $LiNO_3$ demonstrated superior thermal stability, even under severe calcination conditions. © 2000 Academic Press

Key Words: **acrylonitrile; oxidative methylation of acetonitrile; Li/MgO catalysts; Li^+O^- surface species; XRD; XPS; EPR.**

INTRODUCTION

Li/MgO is a promising catalyst for the oxidative coupling of methane and has enticed several researchers to investigate it further. Lunsford and co-workers (1, 2) proposed a mechanism for the oxidative coupling of methane reaction in which the active sites are Li^+O^- species at the surface of the catalyst. It was proposed that methane is activated by hydrogen abstraction, forming methyl radicals. Ethane and ethene are subsequently formed by the coupling of methyl radicals in the gas phase.

In our previous work (3), it was found that Li/MgO, synthesized with MgO and LiCl, is a suitable catalyst for the oxidative methylation of acetonitrile to acrylonitrile with methane. It was shown, however, that this catalyst deactivated with time on stream, as indicated by changes in product selectivity. This deactivation was a direct result of the gradual loss of the active lithium sites. The selectivity of acrylonitrile decreased significantly while the selectivity of carbon dioxide increased with time on stream. Our results (4) also support that Li^+O^- active sites on the catalyst are responsible for the simultaneous formation of methyl and acetonitride radicals, which combine to form propionitrile via Langmuir–Hinshelwood kinetics. Acrylonitrile was subsequently formed by oxidative dehydrogenation of propionitrile.

In the present paper we described the nature and origin of the surface sites of Li on the Li/MgO-based catalysts for oxidative methylation of acetonitrile to acrylonitrile. The results obtained from the activity of catalysts, XRD, and XPS studies are in excellent agreement with the Li^+O^- species identified by EPR. The latter species are responsible for the oxidative methylation of acetonitrile to acrylonitrile.

[1] Department of Chemistry, University of Cincinnati, Cincinnati, OH 45221-0172.

[2] To whom correspondence should be addressed.

0021-9517/00 $35.00

EXPERIMENTAL

Reaction Apparatus and Procedure

Catalyst preparation. The MgO catalyst supports in the present study were prepared by thermal decomposition of the magnesium precursors. This method was selected based on a study by Gardner and Messing (5), in which samples of high surface area MgO were obtained by rapidly heating aerosolized aqueous solutions of various magnesium precursors. The precursors that were used in this study were all purchased from Aldrich Chemicals and include magnesium ethoxide (98%), magnesium acetate tetrahydrate (99%), magnesium carbonate hydroxide (99%), magnesium hydroxide (95%), and magnesium nitrate hexahydrate (98%). Samples of approximately 2 g of each magnesium precursor were placed in a temperature-programmable furnace and were heated at a rate of 50 K/min to a final temperature of 850°C. The samples were held at 850°C for 2 h. They were then cooled at a rate of 50°C/min to 150°C. The resulting MgO supports had BET surface areas ranging from 10 to 55 m^2/g and were used as catalyst supports for Li/MgO catalysts. In addition, commercial MgO (98%, Aldrich Chemicals) was used as a catalyst support for comparison.

A wet impregnation method was used to synthesize the Li/MgO catalysts. These methods were described in detail previously (3). Briefly, the Li/MgO catalysts were prepared by mixing the lithium precursor and magnesia such that the weight concentration of lithium is nominally 20% (based on Li and MgO only). In other words, the Li/MgO weight ratio for all catalysts is 0.25. The appropriate amounts of lithium precursor in distilled water and magnesia were mixed vigorously under heating. The distilled water added to form the slurry was in proportion 1 g of MgO to 60 cm^3 of aqueous solution of the lithium precursor. The slurry was heated and stirred until the water was nearly evaporated. The resulting powder mixture was dried further in an oven at 125°C overnight and subsequently calcined in air at 650°C for 14 h. After calcination, the catalysts were stored in a vacuum drier at 100°C to minimize the adsorption of water and CO_2. The catalysts prepared for this study are presented in Table 1.

Reaction apparatus and procedure. The performance of each catalyst was investigated in a differential packed-bed reactor system. The test system is composed of a $\frac{1}{4}$-in. o.d. high-purity alumina tube reactor (AD998 Coors Ceramics), placed horizontally in a temperature-programmable furnace. The gases for the reaction (4.24% CH_4 in helium, 4.28% O_2 in helium, and balance 99.99% helium) were supplied by three anticorrosive mass flow controllers (MKS). A syringe pump was used to introduce acetonitrile through a heated line into the test system at a predetermined rate. A Varian 3700 gas chromatograph (GC) equipped with both FID and TCD detectors was used for the analyses of the reactor effluent. A series of three GC columns were used for the analyses of the reactor effluent: (1) Supelco Nukol Custom capillary column (50-ft length, 0.53-mm i.d.), (2) 80/100 Haysep Q-packed column (10-ft length, 1/8-in. o.d.), and (3) 45/60 molecular sieve 13X packed column (6-ft length, 1/8-in. o.d.). In this system, the first column separates the nitriles from the light gases, the second column separates methane and CO_2, and the third column separates oxygen, nitrogen, and CO.

TABLE 1

Li/MgO Catalysts Synthesized with Different Li and Mg Precursors for 20 wt% Nominal Composition of Lithium (Based On Li and MgO Only); The Catalysts Were Calcined at 650°C for 14 h in Air

Catalyst	Magnium oxide source	Lithium source	MgO BET surface area (m^2/g)	Catalyst BET surface area (m^2/g)
C1	$Mg(OC_2H_5)_2$	LiCl	55	0.6
C2	$Mg(OC(O)CH_3)_2$	LiCl	24	0.7
C3	MgO from Aldrich	LiCl	10	0.6
C4	$MgCO_3$	LiCl	39	2.2
C5	$Mg(OH)_2$	LiCl	27	1.0
C6	$Mg(NO_3)_2$	LiCl	5	1.2
C7	MgO from Aldrich	Li_2CO_3	10	5.7
C8	MgO from Aldrich	$Li(OC(O)CH_3)$	10	3.4
C9	MgO from Aldrich	LiOH	10	0.4
C10	MgO from Aldrich	$LiNO_3$	10	2.9

For each catalytic experiment, approximately 100 mg (±5 mg) of catalyst (on a dry basis) was loaded into the reactor tube and placed in-between two quartz wool plugs. The catalyst was preconditioned at 450°C with 4.28% oxygen in helium at 15 cm^3/min for 1 h. The temperature of the reactor was then brought up to 680°C, after which the reactants were introduced to initiate the reaction. The reactants were methane, acetonitrile, and oxygen in a molar ratio of 5 : 1.8 : 1, unless otherwise specified. They were introduced into the reactor at a WHSV of 0.8 h^{-1}.

Catalyst Characterization

BET surface area and pore-size distributions. The MgO supports and the Li/MgO catalysts were characterized with respect to BET surface area and pore size distribution by nitrogen adsorption at 77 K using an accelerated surface area and porosity apparatus (ASAP 2010, Micromeritics). Prior to analyses, 0.5–1 g of the MgO supports or catalysts were degassed at 350°C and 200 mm Hg for 4 or more hours. The adsorption isotherms of nitrogen were collected at 77 K using approximately 20 values of relative pressure ranging from 0.05 to 0.99. The pore-size distribution of the MgO supports and Li/MgO catalysts were also measured for catalysts C1–C10. It should be noted, however, that the instrument offers very high accuracy for samples with surface area higher than 10 m^2/g. In this study, the catalyst

samples used for the BET surface area measurements had surface areas of less than 1 m^2/g in most cases, which is outside the manufacturer's recommended range to ensure high accuracy. The BET surface areas of the MgO supports and Li/MgO catalysts are presented in Table 1.

Chemical analyses. Lithium and magnesium concentrations in each catalyst sample were determined using ICP spectroscopy (Model 61E, Thermo Jerrell Ash Corp). Approximately 15 mg of each catalyst was dissolved in 2 vol% HNO_3 prior to the ICP analyses. The ICP instrument was calibrated using prepared standards of MgO and LiCl in 2% nitric acid, ranging in concentrations from 0 to 160 ppm by weight for lithium and from 0 to 650 ppm by weight for magnesium. Chloride concentrations were measured using a gravimetric method (6). This method requires the use of silver nitrate and nitric acid. Dilute nitric acid (2% by volume) was used to dissolve samples of fresh catalysts. Silver nitrate solution was added to aliquots of the dissolved catalyst solutions. The silver ion from $AgNO_3$ reacted with the chloride ion to form AgCl which rapidly precipitated out of solution. The precipitate was collected by filtration, and the filtrate was subsequently dried and weighed. The chloride concentration in the catalyst was determined from the collected weights of AgCl.

XRD studies. The crystallinity of each catalyst was determined using a Siemens X-ray diffractometer using a Cu$K\alpha$ source. X-ray diffraction (XRD) spectra were obtained for the lithium precursors and catalysts for comparison. The *d* values of the main peaks were used to identify the crystal phases and to compare the spectra of the catalysts and lithium precursors. The XRD phases present in the samples were identified with help of JCPDS files.

XPS studies. X-ray photoelectron spectroscopy was used to analyze the atomic surface concentrations on each catalyst. The samples for the XPS studies were prepared as follows. Prior to the XPS measurements all catalysts were calcined at 650°C in dry air for 14 h. The calcined samples were again heated at 680°C for 2 h in 4% oxygen (balance helium). Then, the XPS analyses were conducted on a Perkin–Elmer Model 5300 X-ray photoelectron spectrometer with Mg$K\alpha$ radiation at 300 W. Typically, 89.45 and 35.75-eV pass energies were used for survey and high-resolution spectra, respectively. The effects of sample charging were eliminated by correcting the observed spectra for a Mg 2*p* binding energy value of 50.3 eV. The powdered catalysts were mounted onto the sample holder and were degassed overnight at room temperature and pressures on the order of 10^{-7} Torr. The binding energies and atomic concentrations of the catalysts were calculated via the XPS results using the total integrated peak areas of the Mg 2*p*, Li 1*s*, O 1*s*, and Cl 2*p* regions.

EPR studies. The samples for the EPR studies were prepared as follows. A known amount of catalyst was heated at 680°C for 2 h in 4% high-purity oxygen (balance is helium). The heated samples were immediately immersed in liquid nitrogen. Then, the samples were transferred into a glove box under nitrogen purge before being loaded into EPR quartz tubes. All the samples were prepared the same way and were kept in a glove box under nitrogen before analyzing them.

The EPR spectra were obtained on a Bruker (Billerica, MA) ESP 300 spectrometer outfitted with a TM110 cavity and a Wilmad 50-ml Dewar flask at 77 K. The instrument parameters were 600-G sweep width, 5-mW microwave power, 100-kHz modulation frequency, 1-G modulation amplitude, 163-ms conversion time, and 20.5-ms time constant. The $g_\perp$ value of 2.0544 corresponding to the $[Li^+O^-]$ signal was determined relative to a paramagnetic Cr^{3+} standard prepared according to a published procedure (7). The peak-to-peak height of the signal at $g_\perp = 2.0544$ was measured and then normalized with respect to the C2 sample for determing the relative $[Li^+O^-]$ amount in the various catalyst samples.

Thermal stability experiments. Thermogravimetric analyses (TGA) were conducted on a Perkin–Elmer TAS 7 TGA apparatus to determine the thermal stability of the catalysts and to quantify the weight loss at elevated temperatures. The TGA analyses were conducted isothermally at 730°C and atmospheric pressure for all catalysts. A continuous stream of nitrogen was used to purge off-gases from the TGA electronics and sample region. The initial amount of each catalyst used for the TGA analyses was approximately 15 mg.

RESULTS AND DISCUSSION

The primary scope of this work was to study the effect of the surface properties and effects of various magnesium oxide and lithium precursors on the synthesis of Li/MgO catalysts for the oxidative methylation of acetonitrile to acrylonitrile.

Catalyst Performance in the Oxidative Methylation of Acetonitrile to Acrylonitrile

Several experiments were conducted to assess the effects of the magnesium oxide and lithium precursors and the catalyst surface properties on the catalyst performance in the oxidative methylation of acetonitrile. A summary of the catalytic performance of all the samples after 2 h on stream under identical operating conditions is shown in Table 2. All catalysts have the same nominal Li composition (20 wt%). The data presented in Table 2 represent averages of at least three replicate experiments. As shown in Table 2, the performance of catalysts C1–C6 for the oxidative methylation of acetonitrile is similar, suggesting that catalyst performance is independent of the source and surface area of the MgO support. A comparison of catalysts

TABLE 2

Summary of Catalyst Performance Experiments for the Oxidative Methylation of Acetonitrile to Acrylonitrile with Methane (CH_4/Acetonitrile/O_2 Molar Ratio of 5 : 1.8 : 1; 100 mg of Catalyst; WHSV = 0.8 h^{-1}; 680°C; 2 h on Stream)

Catalyst sample	Lithium precursor	Acetonitrile conversion (%)	Selectivity (wt%)			
			Acrylonitrile	Propionitrile	Carbon dioxide	Carbon monoxide
C1	LiCl	46	29	<3	71	0
C2	LiCl	46	26	<3	72	0
C3	LiCl	47	30	<3	70	0
C4	LiCl	51	28	<3	70	0
C5	LiCl	54	28	<3	69	0
C6	LiCl	45	33	<3	65	0
C7	Li_2CO_3	60	12	0	63	24
C8	$LiOC(O)CH_3$	64	15	<3	58	26
C9	LiOH	61	22	<3	74	0
C10	$LiNO_3$	63	13	<3	64	23

C3 and C7–C10 shows that the lithium precursor has a significant effect on the performance of the catalyst for the formation of acrylonitrile. It should be noted that catalyst C3 was used in our previous work (3, 4). In addition, a comparison of the performances of C3 and C9 suggests that LiCl and LiOH precursors result in catalysts with comparable properties for this reaction. As will be shown later in this paper, the lithium precursor has a significant effect on the concentration and form of lithium on the surface of the catalyst, and it will affect the availability of Li^+O^- active sites on the catalyst. Others (8) made a similar observation in the oxidative coupling of methane, which suggested that the selectivity and activity of Li/MgO catalysts are a function of the concentration of Li^+O^- active sites on the surface of the catalyst.

It is also noted (Table 2) that C7, C8, and C10 have much lower selectivities for acrylonitrile than C1–C6 and C9 catalysts. We attribute this behavior to the existence of relatively low concentrations of Li on the surface of the former catalysts. Moreover, lithium is in the form of Li_2CO_3 on the surface of those catalysts, which is relatively inactive compared to Li^+O^- active sites of the latter catalysts. Camino *et al.* (9) also observed relatively low activity and selectivity for C_2 hydrocarbons in the oxidative coupling of methane reaction with Li/MgO catalysts prepared with Li_2CO_3. It is likely that Li_2CO_3 does not decompose on the surface of the catalysts at the reaction temperatures, thus preventing the formation of active Li^+O^- sites.

Finally, it was observed that the acetonitrile conversions were slightly higher with catalysts that were not synthesized with LiCl (catalysts C7, C8, and C10) than with the LiCl/MgO catalysts (C1–C6) and LiOH (C9). As noted in Tables 1 and 3, with the exception of C9 (LiOH/MgO), the higher acetonitrile conversion corresponds to catalysts with higher BET surface areas, lower acrylonitrile selectivities, and formation of significant amounts of CO. Catalysts C7, C8, and C10, having larger surface areas than catalysts C1–C6 and C9, may have available active sites at 680°C that favor the formation of CO and CO_2.

Fresh Catalyst Characterization

The catalysts were characterized with respect to BET surface area and pore-size distribution. Originally, it was expected that by developing a high surface area Li/MgO catalyst, the number and availability of Li^+O^- sites at the surface would increase, thus resulting in improved catalytic performance for the oxidative methylation of acetonitrile. As shown in Table 1, the BET surface areas of the catalysts were relatively low compared to the surface areas of the MgO supports. The BET surface areas of the MgO supports for catalysts C1–C6 ranged from 10 to 55 m^2/g. The organic

TABLE 3

Summary of Results of ICP Analyses of Li/MgO Catalysts with 20 wt% Nominal Composition of Lithium (Based on Li and MgO Only); The Catalysts Were Calcined at 650°C in Air for 14 h

Catalyst sample	Lithium concentration (wt%)		Magnesium concentration (wt%)	
	Measured	Expected	Measured	Expected
C1	11.4	9.9	27.8	23.9
C2	11.0	9.9	27.5	23.9
C3	10.3	9.9	26.3	23.9
C4	10.2	9.9	25.8	23.9
C5	10.6	9.9	24.8	23.9
C6	10.6	9.9	27.4	23.9
C7	12.2	10.7	27.9	25.9
C8	12.2	10.7	26.6	25.9
C9	10.2	11.4	40.8	34.8
C10	14.6	11.4	42.3	34.8

Note. The weight percentages of Li and Mg are based on the weight concentrations of four elements (Li, Mg, O_2, and Cl_2).

magnesium salts and magnesium carbonate yielded samples of MgO with relatively high surface areas. However, the MgO prepared by rapidly heating $Mg(NO_3)_2$ had a BET surface area very similar to that of the purchased MgO. In each case, the addition of LiCl to the MgO support significantly decreased the surface area of the MgO support to less than 2 m^2/g. Significant reduction in BET surface area of the commercial MgO (10 m^2/g) was also observed upon the addition of other lithium salts. Other researchers (10) also observed a reduction in BET surface area after the addition of lithium. They attributed the reduction in surface area to the lithium salts forming a mobile liquid phase on the surface of the MgO support which fuses and forms large crystals upon cooling. The MgO support purchased from Aldrich had a pore-size distribution with a maximum at a pore size of approximately 2 nm. The MgO supports prepared by thermal oxidation of magnesium precursors had pore-size distributions maxima in the range of 10–12 nm; a few samples demonstrated bimodal distribution with maxima at 2 and ~10 nm.

The fresh catalysts contain between 10 and 15 wt% lithium and between 25 and 43 wt% magnesium (Table 3). It should be noted that the weight percentages of Li and Mg are based on the weight percentages of four elements (Li, Mg, O_2, and Cl_2). The measured Li and Mg weight percentages compare well with those expected. The expected weights of Li and Mg in the catalysts were based on the amounts of magnesium and lithium precursor used to synthesize the catalysts, assuming no Li or Mg losses during synthesis. It is remarkable to note (Table 4) that the chloride concentration of catalysts synthesized with LiCl (C1–C6) range from 40 to 50 wt%. These data indicate that chloride remains in the catalysts during synthesis at subsequent calcination. As will be shown below in detail, both XRD and XPS analyses indicate that Li and Cl are predominantly in the form of LiCl for all the LiCl/MgO catalysts (C1–C6).

XRD Results

XRD analysis of the catalysts and of the magnesium and lithium precursors indicate that the catalysts are predominantly mixtures of the lithium precursors or decomposition products of the precursors (e.g., LiCl, Li_2CO_3, and LiOH) and MgO.

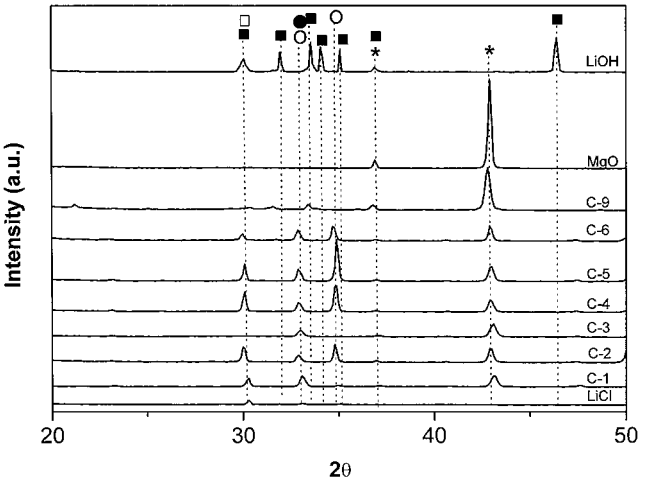

FIG. 1. XRD of C1–C6, C9, and corresponding Li precursors and magnesium oxide (∗ corresponds to MgO, ○ corresponds to Li_2O_2, □ corresponds to LiCl, ■ corresponds to LiOH, and ● corresponds to $LiClH_2O$).

XRD patterns of the lithium chloride, lithium hydroxide, and magnesium oxide and their corresponding catalysts C1–C6 and C9 calcined at 650°C in an air atmosphere are shown in Fig. 1. One can observe from this figure that the C2, C4, C5, and C6 catalysts possess sharp diffraction lines at 2θ values of 34.9° and 32.9° which correspond to Li_2O_2 (JCPDS card no. 9-0355) phase. The formation of a Li_2O_2 peak results from the partial decomposition of LiCl of the catalysts C2, C4, C5, and C6 when they are calcined at 650°C in an air atmosphere. It is important to note that the hydrated form of LiCl and Li_2O_2 both contributed to the peak at $2\theta = 32.9°$. Only weak diffraction peaks at 2θ values of 42.9° and 30.06° corresponding to the MgO and LiCl, respectively, can be seen. The observed Li_2O_2 compound formation may presumably be due to different precursor compounds used for the preparation of the above catalysts in the present study.

XRD patterns of the lithium precursors (LiCl, LiOH, and Li_2CO_3), magnesium oxide, and their catalysts C1 and C7–C10 calcined at 650°C are shown in Fig. 2. As can be noted from this figure, C7–C10 catalyst samples containing diffraction lines at 2θ values of 36.8°, 36.0°, 34.2°, 31.8°, 30.7°, 29.4°, and 21.2° are due to the formation of lithium carbonate. This is as expected since lithium carbonate was itself used as a precursor in the case of C7 catalysts and a lithium acetate precursor was decomposed into lithium carbonate upon calcination in the case of C8 catalysts. It is remarkable to note that catalysts synthesized with $LiNO_3$ demonstrated thermal stability due to the decomposition of $LiNO_3$ to Li_2O (XRD peak at 33.6° of JCPDS no. 12-0254). Li_2CO_3 was also formed on the surface of C10 during

TABLE 4

Results of Gravimetric Chloride Analyses Using $AgNO_3$ (Jeffery and Hutchison, 1981) of Li/MgO Catalysts Quantisized with 20 wt% Nominal Composition of Lithium Based on Li and MgO Only; The Catalysts Were Calcined at 650°C in Air for 14 h

Catalyst sample	Measured chloride (wt%)	Expected chloride (wt%)	Ratio measured/expected
C1	44	50.5	0.88
C2	40	50.5	0.79
C3	51	50.5	1.02
C4	45	50.5	0.88
C5	48	50.5	0.95
C6	40	50.5	0.80

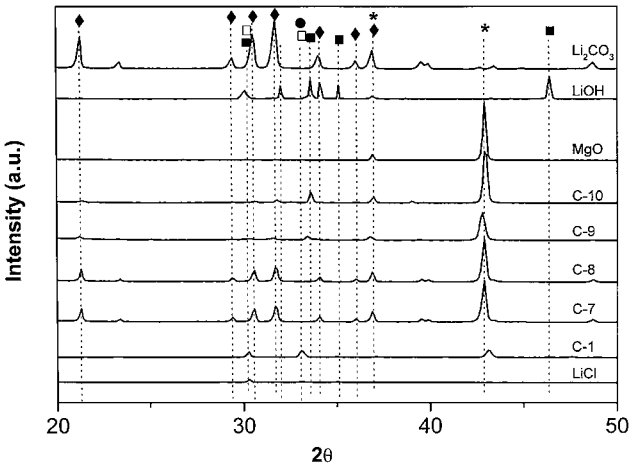

FIG. 2. XRD of C1, C7–C10, and corresponding Li precursors and magnesium oxide (∗ corresponds to MgO, □ corresponds to LiCl, ■ corresponds to LiOH, ◆ corresponds to Li_2CO_3, and ● corresponds to $LiClH_2O$).

calcination at 650°C. Most importantly, no lines due to Li_2O_2 are seen in those spectra (Fig. 2). This observation clearly indicates that the precursors used in the catalysts C7, C8, and C10 were not decomposed into Li_2O_2. For the C9 catalyst no peaks corresponding to Li^+O^- species were detected by XRD. From the surface characterization presented below and the catalytic tests, we concluded that the latter catalyst does possess small amounts of Li^+O^-. However, the corresponding XRD band for the latter species is very weak. A closer look into Figs. 1 and 2 reveals that the MgO peak at a 2θ value of approximately 42.9° is present in all catalysts, and it is the dominant peak in catalysts C7–C10.

XPS Results

Catalysts C1–C10 were characterized by XPS technique after calcination and, again, after a second heat treatment. It should be mentioned that the calcination step was conducted at 650°C in air. The second heat treatment step was conducted at 680°C in 4% oxygen (balance helium). This second heat treatment step was performed to simulate the *in situ* catalyst activation conditions carried out prior to the catalytic experiments. The heated samples were immediately immersed in liquid nitrogen to "freeze" the active sites and lattice defects of the samples which can act as catalytic sites. Lunsford and co-workers (1, 2) used the same procedure to form and stabilize Li^+O^- species of Li/MgO catalysts. Then, the samples were kept in a glove box under nitrogen purge until XPS analyses were performed. The XPS analyses of catalysts C1–C6 before the second heat treatment indicate that MgO and LiCl are present on the surface of the catalyst. This is supported by the atomic ratios of Li : Cl and Mg : O being 1 : 1 and 1 : 2 (not shown), respectively. However, after the second heat treatment of these samples, the ratio of Li : Cl increased to more than 1 and the ratio of Mg : O reduced to 1 : 1 as shown in Table 5. It should be noted that the atomic Mg : O ratio for catalysts C2 and C6 is less than the case of C1, C3, C4, and C5 due to the additional oxygen atoms contained in the magnesia precursors. This interesting variation in these ratios is due to the volatilization of chloride and the formation of Li^+O^- (Li_2O_2) species on the surface of the catalysts under the conditions of the second heat treatment. For catalysts C7–C10, the Mg : O ratios after the second heat treatment vary from catalyst to catalyst. However, the ratio becomes significantly lower (less than 0.5) for the case of catalysts C7–C10 after the second heat treatment. This result is because of the presence of additional oxygen introduced by the lithium precursors.

The photoelectron peaks of Li 1*s* and Mg 2*p* for all catalysts after the second heat treatment are depicted in Fig. 3. The binding energy values for Li 1*s* and Mg 2*p* core levels for all catalysts after the heating treatment are presented

TABLE 5

Summary of Atomic Concentration at the Surface of the Catalysts after Heat Treatments at 680°C for 2 h under Oxygen Flow Determined by XPS (Mg$K\alpha$ Radiation at 300 W, 89.45- and 35.75-eV Pass Energies)

Catalyst sample	Lithium precursor	Atomic concentrations (%)					
		Lithium	Chlorine	Li/Cl	Magnesium	Oxygen	Mg/O
C1	LiCl	26.18	23.35	1.121	25.78	24.69	1.044
C2	LiCl	17.34	23.30	0.744	20.08	39.28	0.511
C3	LiCl	31.09	26.54	1.171	20.92	21.45	0.975
C4	LiCl	30.41	27.80	1.223	21.66	20.13	1.076
C5	LiCl	24.77	19.20	1.290	27.85	28.17	0.988
C6	LiCl	34.08	28.88	1.180	15.67	21.37	0.733
C7	Li_2CO_3	23.50	0	NA	11.24	65.26	0.172
C8	$LiOC(O)CH_3$	18.91	0	NA	19.28	61.81	0.312
C9	LiOH	35.06	0	NA	6.30	58.64	0.107
C10	$LiNO_3$	29.17	0	NA	9.16	61.67	0.148

Note. NA stands for not applied.

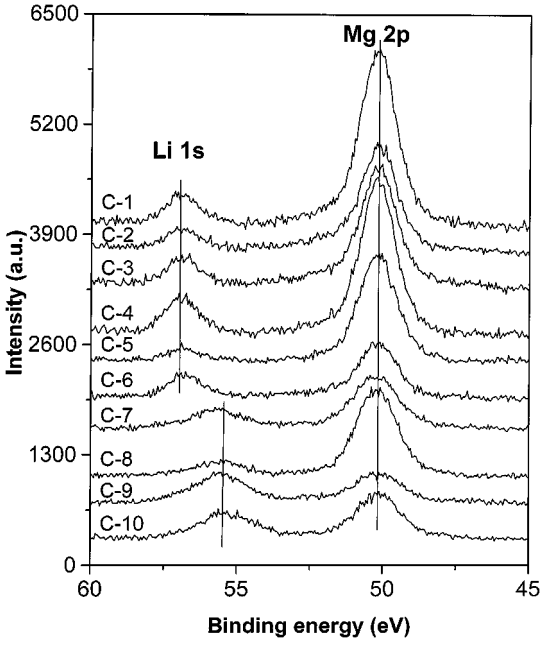

FIG. 3. XPS of Mg 2*p* and Li 1*s* peaks for C1–C10 catalysts (Mg$K\alpha$ radiation at 300 W, 89.45- and 35.75-eV pass energies).

in Table 6. In all XPS spectra the Mg 2*p* is the most intense peak. This peak does not depend on the charging effect of the source and seems to remain in the same chemical state for all the samples. Hence, Mg 2*p* at 50.3 eV was considered to be a good reference for binding energy calibration (11). From the data presented in Fig. 3 and Table 6 one can clearly observe that the binding energy values of Li 1*s* varied between 55.3 and 57.0 eV. This can be explained by the fact that different lithium precursors were used during the preparation of the above samples. The intensities of Mg 2*p* and Li 1*s* peaks varied from sample to sample as shown in Fig. 3. The intensities of the Li 1*s* peak is relatively weak for catalysts C7, C8, and C10. This agrees very well with the relatively poor catalytic behavior of these samples (Table 2). We observed the formation of lithium carbonate on the surface of the C7 and C8 was expected since they were synthesized from lithium carbonate and lithium acetate. The intensity of the Li_2CO_3 peak (55.5 eV) (12) was relatively large for the C9 catalysts. This was not as expected since the catalyst C9 was prepared with MgO and LiOH and no carbon-containing precursors. This behavior was reproduced repeatedly with numerous C9 catalysts synthesized under identical conditions. It is likely that lithium carbonate was formed on the surface of the catalyst during calcination in the presence of air. Similarly, we observed Li_2CO_3 for C10, even though one would expect to observe $LiNO_3$. The N 1*s* peak at 407 eV was not observed at all, thus indicating that the $LiNO_3$ decomposed completely.

We performed deconvolution of the XPS spectra of C2 (representative of LiCl/MgO catalysts C1–C6), C8 (representative of Li_2CO_3/MgO catalysts C7 and C8, $LiNO_3$/MgO catalysts C10), and C9 (representative of LiOH/MgO) catalyst samples to obtain the peak intensity of Li^+O^- (Li_2O_2) species, presented in Fig. 4. This sorting of the samples was based on their catalytic behavior. The XPS spectra of the C2 catalyst shows that the Li 1*s* spectra consisted of three different peaks corresponding to Li_2O_2 (57.0 eV), LiCl (56.0 eV) (13), and Li metal (52.3 eV) (14). The Mg 2*p* spectra were assigned to MgO (50.3 eV) (11) and $Mg(OC(O)CH_3)_2$ (51.2 eV). LiCl and $Mg(OC(O)CH_3)_2$ were used as a

TABLE 6

Binding Energy Values of Li 1*s* and Mg 2*p* Core Levels for C1–C10 Catalysts after a Second Heat Treatments at 680°C for 2 h under Oxygen Flow (Mg$K\alpha$ Radiation at 300 W, 89.45- and 35.75-eV Pass Energies)

Catalyst sample	Binding energy (eV)	
	Mg 2*p*	Li 1*s*
C1	50.3	56.9
C2	50.3	57.0
C3	50.3	57.1
C4	50.3	56.9
C5	50.3	57.1
C6	50.3	57.0
C7	50.3	55.6
C8	50.3	55.5
C9	50.3	55.6
C10	50.3	55.3

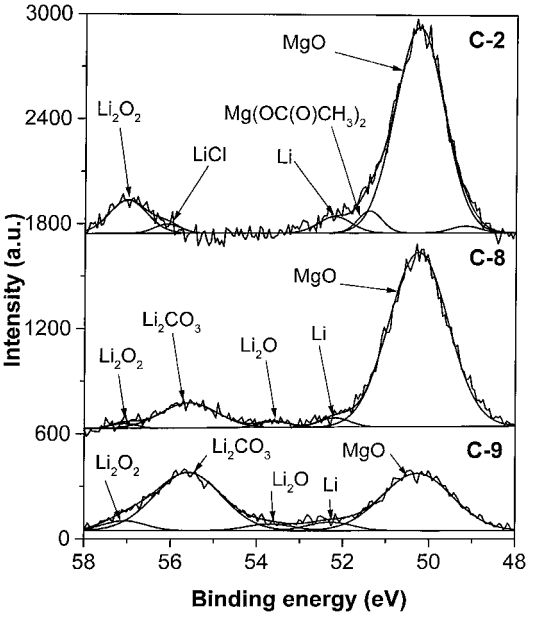

FIG. 4. XPS deconvolution of Mg 2*p* and Li 1*s* peaks for C2, C8, and C9 catalysts (Mg$K\alpha$ radiation at 300 W, 89.45- and 35.75-eV pass energies). The peaks presented are Li_2O_2 (57.0 eV), LiCl (56.0 eV), Li_2CO_3 (55.5 eV), Li_2O (53.7 eV), Li metal (52.7 eV), $Mg(OC(O)CH_3)_2$ (51.4 eV), and MgO (50.3 eV).

TABLE 7

Weight Percents from XPS Analyses for the Catalysts after a Second Heat Treatment at 680°C for 2 h under Oxygen Flow (Mg$K\alpha$ Radiation at 300 W, 89.45- and 35.75-eV Pass Energies)

Catalyst sample	Lithium precursor	Weight concentrations (%)			
		Lithium	Chlorine	Magnesium	Oxygen
C1	LiC1	9.0	40.8	30.7	19.5
C2	LiC1	9.1	43.2	28.5	19.2
C3	LiC1	10.7	46.8	25.3	17.2
C4	LiC1	10.3	48.2	25.7	15.8
C5	LiC1	9.0	34.3	34.2	22.5
C6	LiC1	11.6	52.7	18.9	16.8
C7	Li_2CO_3	11.0	0	18.5	70.5
C8	$LiOC(O)CH_3$	8.3	0	29.4	62.3
C9	LiOH	18.2	0	11.5	70.3
C10	$LiNO_3$	14.3	0	15.8	69.9

precursor for the synthesis of the C2 catalyst. In this spectra the intensity of the Li_2O_2 peak is stronger than that of LiCl and Li metal. To the best of our knowledge there is no previous communication dealing with Li 1*s* binding energy for the Li^+O^- (Li_2O_2) species. The formation of Li^+O^- species may occur due to substitution effects on the MgO lattice with LiCl and LiOH while heating at elevated temperatures in an oxygen stream. Due to these interfacial effects between the already formed Li_2O_2 and MgO support, for every Li^+O^- center a nearest neighbor Mg^{2+} becomes more positive ($Mg^{2+\delta+}$) which shifts the Li^+O^- peak to a higher binding energy, namely, 57.0 eV. From our EPR results below we concluded this new XPS peak at 57.0 eV corresponds to the Li^+O^- species. The case of $LiClO_4$ (57.2 eV) (13) should be excluded because the low oxygen levels (rows 1–6) measured by XPS (Tables 5 and 7) cannot justify the existence of $LiClO_4$. From Fig. 4, one can observe that the C8 sample possesses four peaks which correspond to Li_2O_2 (57.0 eV), Li_2CO_3 (55.5 eV), Li_2O (53.7 eV) (14), and Li metal (52.3 eV). Comparable peaks, for the latter four species, were determined for the C9 sample. The intensity of Li_2CO_3 is stronger than that of Li_2O_2, Li_2O, and Li metal in C8 and C9 catalysts. However, the intensity of Li_2O_2 for the C2 catalyst is stronger than that of C9, followed by C8. Moreover, the presence of Li_2O_2 on the surface of C2 and Li_2CO_3 on the surface of C8 and C9 catalysts has been verified by XRD. Hence, XPS results suggest that the catalysts prepared with LiCl and LiOH as precursors are active for the oxidative methylation of acetonitrile to acrylonitrile due to the presence of Li_2O_2 on the surface of these catalysts.

The compositions of the surface of all catalysts are shown in Table 7. The C1–C6 catalysts keep the lithium concentration on the surface very comparable due to the fact that LiCl was used as the precursor. The lithium concentration of C7 is comparable to that of the above catalysts since the melting points of LiCl and Li_2CO_3 are comparable (605 and 723°C, respectively). However, this is not the case with C8 where the surface lithium concentration drops significantly. We believe this is due to the low melting point (70°C) of lithium acetate used during the synthesis of the C8 catalysts. The surface concentration of lithium for C9 was found repeatedly to be high. By observing the bulk lithium concentration detected by ICP, we conclude that lithium migration to the surface takes place. A high lithium concentration for C10 was observed at both the surface and bulk due to the stable nature of Li_2O formed from $LiNO_3$ decomposition. This claim is supported by the TGA studies reported below. At this point it should be noted that the catalyst performance for the production of acrylonitrile does not depend directly on the Li surface concentration. The C7 and C10 catalysts had equal or more lithium than that of the active catalysts, but their catalytic performance was inferior due to the lack of Li^+O^- species.

XPS analysis also indicated that the catalyst C9 (LiOH/MgO) had a significant concentration of Li_2CO_3 on its surface. However, the selectivity of C9 for acrylonitrile was comparable to the performance of LiCl/MgO catalysts because of its comparable surface concentration of Li^+O^- species. Similar activities for catalysts C1–C6 and C9 for the oxidative methylation of acetonitrile suggest that the chloride in the catalysts prepared with LiCl/MgO does not seem to play a role for this reaction. Lunsford and co-workers (15) observed that the Li : Cl ratio in the catalyst significantly affects the performance of the catalyst for the oxidative coupling of methane over Li/MgO. In that study (15), it was found that the best catalyst performance was obtained when the ratio of Li : Cl was 1 : 1.

EPR Results

The paramagnetic center of $[Li^+O^-]$ characterized by its $g_\perp = 2.0544$ (16) was used to determine the relative amount of $[Li^+O^-]$ in the various samples by EPR at 77K. Typical EPR spectra are shown in Fig. 5 where the arrow marks the position of $g_\perp = 2.0544$. For example, sample C8 displays no signal under the arrow while a distinct signal is observed with C9. The percentage of $[Li^+O^-]$ in the various samples relative to that of C2 (arbitrarily set at 100%) is shown in Fig. 6. The signal described here was very stable in all samples except in the case of C3 which displayed some dynamic behavior. It is remarkable to note that C7, C8, and C10 catalysts do not possess any Li^+O^- species as indicated in Fig. 6. This agrees completely with the catalytic results presented in Table 2 where the acrylonitrile selectivity was relatively low and that for CO was relatively high. The rest of the samples possessed Li^+O^- species ($g_\perp = 2.0544$), which agrees with the relatively high selectivity of acrylonitrile selectivity and the absence of CO. The results obtained from EPR spectra are in excellent agreement with the XPS results explained in earlier paragraphs.

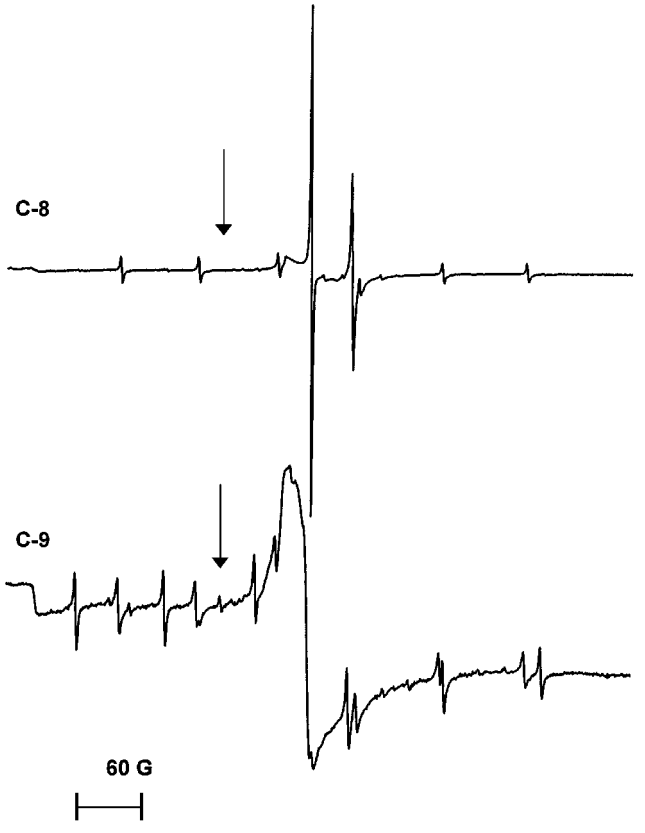

FIG. 5. EPR spectra of samples C8 and C9 at 77 K. Position of arrows corresponds to $g_{\perp} = 2.0544$.

Catalyst Stability

Catalyst stability was investigated for each catalyst prepared for this study by conducting time-on-stream experiments and by investigating the thermal stability via thermo-

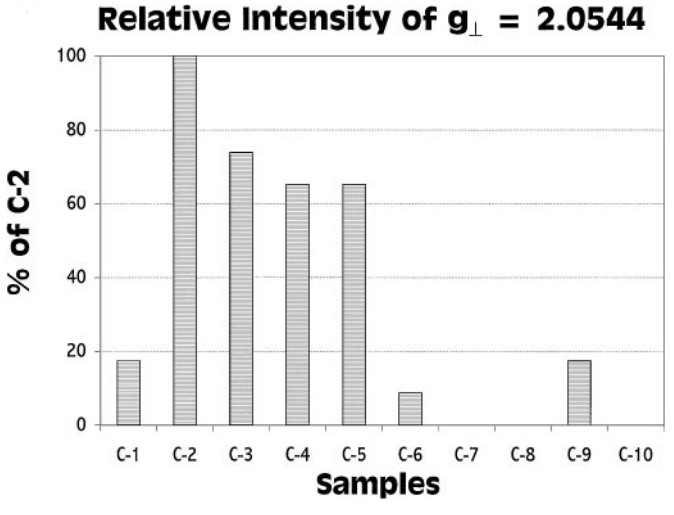

FIG. 6. Bar graph displaying the relative amount of $[Li^+O^-]$ in the catalyst samples C1–C10 with respect to that of C2 catalyst based on the signal intensity at $g_{\perp} = 2.0544$.

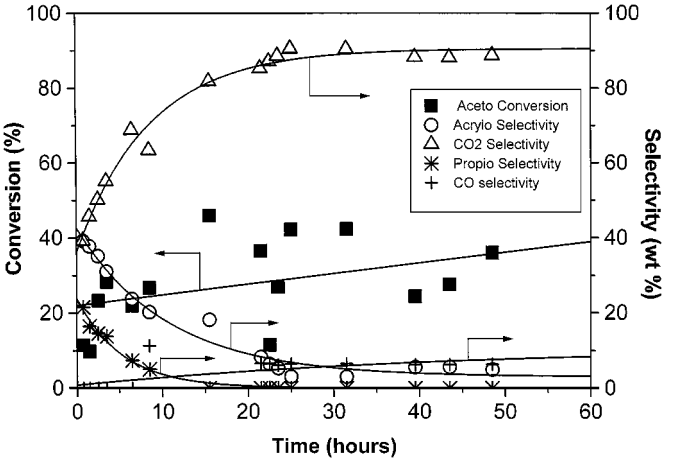

FIG. 7. Acetonitrile conversion and product selectivities as a function of time on stream. For LiCl/MgO catalyst (C2) (CH_4/acetonitrile/O_2 molar ratio of 5 : 1.8 : 1; 100 mg of catalyst, WHSV = 0.8 h^{-1}; 680°C).

gravimetric analyses of the catalysts. The time-on-stream (TOS) behavior of catalysts prepared with lithium chloride and magnesium oxide were investigated by performing the reaction for approximately 60 h with a representative catalyst (C2). These catalysts were selected because they demonstrated the best performance after 2 h on stream. Figure 7 graphically shows the TOS behavior of these catalysts. The time-on-stream behavior in this study for C2 confirms the results reported previously (4) for LiCl/MgO catalysts. C2 is active due to the formation of Li^+O^- during the calcination of the catalyst samples in oxygen. In the case of C2, XRD data show that the peaks corresponding to Li_2O_2 ($2\theta = 34.9°$, 32.9°) are the dominant ones, unlike with other catalysts where the peaks which correspond to MgO, Li_2CO_3, and Li_2O are dominant. It was observed that the acrylonitrile selectivity decreases, while the selectivity of CO_2 increases with time on stream as a result of catalyst deactivation.

The cause of this behavior with the Li/MgO catalyst is the loss of lithium from the catalyst support, as will be shown later in this paper by TGA data and ICP analyses of fresh and used catalysts after 2 h. Perrichon and Durupty (10) proposed that lithium sublimation is the possible mechanism for the loss of lithium from Li/MgO catalysts. Their data suggested that reaction with the surfaces of the reactor was the most probable loss mechanism for lithium, as indicated by the noticeable activity of the reactor walls to the oxidative coupling of methane (10). In our study, sublimation of Li was observed. Deposits recovered from the post reaction zone of the reactor were found to be lithium (3). Evidence for this decomposition of the Li precursors was demonstrated by bubbling the reactor effluent through a solution of silver nitrate. The observation of silver chloride precipitating in the solution after 3 h on stream, though qualitative, suggests that the chloride eludes from the

TABLE 8

Comparison of Lithium and Magnesium Concentrations as Determined by ICP Analyses of Li/MgO Catalysts (20 wt% Nominal Composition of Lithium Based on Li and MgO Only) Prior to Use and after 2 h on Stream (CH_4/Acetonitrile/O_2 Molar Ratio of 5 : 1.8 : 1; 100 mg of Catalyst; WHSV = 0.8 h^{-1}; 680°C)

Catalyst sample	Lithium (wt%)			Magnesium (wt%)		
	Fresh	Tested for 2 h	Ratio tested/fresh	Fresh	Tested for 2 h	Ratio tested/fresh
C1	11.4	9.1	0.80	27.8	30.3	1.1
C2	11.0	8.4	0.76	27.4	23.3	0.85
C3	10.3	7.4	0.72	26.3	31.7	1.2
C4	10.2	10.1	0.99	25.8	24.6	0.95
C5	10.6	8.7	0.82	24.8	29.3	1.2
C6	10.6	7.1	0.67	27.9	30.4	1.1
C7	12.2	7.1	0.58	27.4	37.1	1.4
C8	12.2	9.0	0.74	26.6	36.1	1.4
C9	10.2	7.1	0.70	40.8	44.5	1.1
C10	14.6	11.1	0.76	42.3	49.7	1.2

Note. The ratio of used-to-fresh magnesium percentage for C2 and C4 catalysts is smaller than 1. This can be explained if one considers that the tested catalysts contain small amounts of quartz wool.

catalyst to some extent in the vapor phase. The loss of lithium from the catalysts was also verified by ICP analyses of fresh and used catalysts after 2 h on stream. Table 8 summarizes the ICP analyses of fresh and used catalysts for lithium and magnesium. By comparing the ratios of the measured lithium and magnesium concentrations for fresh and used catalysts, we observed a relative decrease of the Li content. Isothermal TGA analyses of each catalyst conducted at 730°C under a nitrogen atmosphere and subsequent ICP analyses of the residual catalysts also indicate a loss of lithium from the catalysts. ICP analyses of the residual catalyst samples, shown in Table 9, indicate that the weight loss was, indeed, a result of the loss of LiCl. A similar behavior was observed with the Li_2CO_3 precursors. Less weight loss was observed for catalysts prepared with $LiOC(O)CH_3$ and LiOH. It is remarkable to note that catalysts synthesized with $LiNO_3$ did not lose any Li. However, this catalyst due to the lack of Li^+O^- species (Fig. 6) was not active for the methylation of acetonitrile to acrylonitrile. The isothermal TGA analyses and subsequent ICP analyses of the residual catalysts from the TGA experiments indicate that the LiCl/MgO catalysts are the least thermally stable among all the catalysts tested in this study.

TABLE 9

Summary of Results from Isothermal TGA and ICP Analyses (Isothermal TGA Experiments at 730°C Using 15 mg of Catalyst)

Catalyst sample	Lithium (wt%)		
	Fresh	After ~20 h at 730°C	Ratio tested/fresh
C1	11.4	0.50	0.04
C2	11.0	0.21	0.02
C3	10.3	0.19	0.02
C4	10.2	0.19	0.02
C5	10.6	0.26	0.02
C6	10.6	0.40	0.04
C7	12.2	0.27	0.02
C8	12.2	7.8	0.64
C9	10.2	6.5	0.64
C10	14.6	15	1.0

CONCLUSIONS

The catalytic performance for the oxidative methylation of acetonitrile to acrylonitrile with methane is virtually independent of the magnesia source and its surface area. The incorporation of lithium to the catalyst supports results in a significant loss of surface area. The performance of the Li/MgO catalysts is significantly affected by the lithium precursor used in catalyst synthesis. The catalysts synthesized with LiCl appear to perform better than those synthesized with other lithium salts. The lithium species at the surface of the catalyst appears to be significant with respect to catalyst performance. The chloride ion does not play a significant role in the oxidative methylation of acetonitrile. This conclusion results from the fact that all samples synthesized with LiCl show very similar behavior to that of a LiOH sample for identical lithium nominal loadings. The loss of LiCl during the reaction is the reason for catalyst deactivation. This is supported by several techniques used in the present study. XPS results suggested that the presence of Li^+O^- species on the surface of LiCl/MgO (C1–C6) and LiOH/MgO (C9) catalysts are responsible for the activity of oxidative methylation of acetonitrile to acrylonitrile. To the best of our knowledge this is the first report of Li^+O^- (57.0 eV) species by the XPS technique. Our results obtained from XRD, XPS, and EPR techniques suggested that the high Li surface concentrations do not necessarily result in effective catalysts for the oxidative methylation of acetonitrile to acrylonitrile. With the exception of catalysts synthesized from $LiNO_3$ (C10), the Li/MgO catalysts deactivated with time on stream. The catalytic behavior of the catalyst prepared with $LiNO_3$ and MgO for the above reaction is relatively poor, even though its thermal stability is relatively high. This behavior agrees completely with the absence of Li^+O^- species observed by EPR.

ACKNOWLEDGMENT

The authors wish to thank BP Chemicals, Inc. for supporting this work and allowing the publication of these findings.

REFERENCES

1. Ito, T., Wang, J.-X., Lin, C.-H., and Lunsford, J. H., *J. Am. Chem. Soc.* **107**, 5062 (1985).

2. Lin, C.-H., Ito, T., Wang, J.-X., and Lunsford, J. H., *J. Am. Chem. Soc.* **109**, 4808 (1987).
3. Zhang, W., and Smirniotis, P. G., *J. Catal.* **182**, 70 (1999).
4. Smirniotis, P. G., and Zhang, W., *Appl. Catal. A* **176**, 63 (1999).
5. Gardner, T. J., and Messing, G. L., *Am. Ceram. Soc. Bull.* **63**, 1498 (1984).
6. Jeffery, P. G., and Hutchison, D., "Chemical Methods of Rock Analysis" Pergamon, New York, 1981.
7. Bobst, A. M., Ireland, J. C., and Bobst, E. V., *J. Biol. Chem.* **259**, 2130 (1984).
8. Korf, S. J., Roos, J. A., Veltman, L. J., Van Ommen, J. G., and Ross, J. R. H., *Appl. Catal.* **56**, 119 (1989).
9. Camino, J. I., Holgado, M. J., and Rives, V., *React. Kinet. Catal. Lett.* **48**, 455 (1992).
10. Perrichon, V., and Durupty, M. C., *Appl. Catal.* **42**, 217 (1988).
11. Ardizzone, S., Bianchi, C. L., Fadoni, M., and Vercelli, B., *Appl. Surf. Sci.* **119**, 253 (1997).
12. Kanamura, K., Tamura, H., Shiraishi, S., and Takehara, Z., *Electrochem. Acta* **40**, 913 (1995).
13. Wagner, C. D., Riggs, W. M., Davis, L. E., Moulder, J. F., and Muilenberg, G. E., "Handbook of X-ray Photoelectron Spectroscopy." Perkin–Elmer Corporation, Physics Electronic Division, Eden Praire, MN, 1978.
14. Shiraishi, S., Kanamura, K., and Takehara, Z-I., *J. Appl. Electrochem.* **29**, 869 (1999).
15. Lunsford, J. H., Hinson, P. G., Rosynek, M. P., Shi, C., Xu, M., and Yang, X., *J. Catal.* **147**, 301 (1994).
16. Driscoll, D. J., Martin, W., Wang, J.-X., and Lunsford, J. H., *J. Am. Chem. Soc.* **107**, 58 (1985).